STRUCTURAL
BIOLOGY

Volume 75 (2019)

Supporting information for article:

Crystal structures of pyrrolidone-carboxylate peptidase I from *Deinococcus radiodurans* reveal the mechanism of L-pyroglutamate recognition

Richa Agrawal, Rahul Singh, Ashwani Kumar, Amit Kumar and Ravindra D. Makde

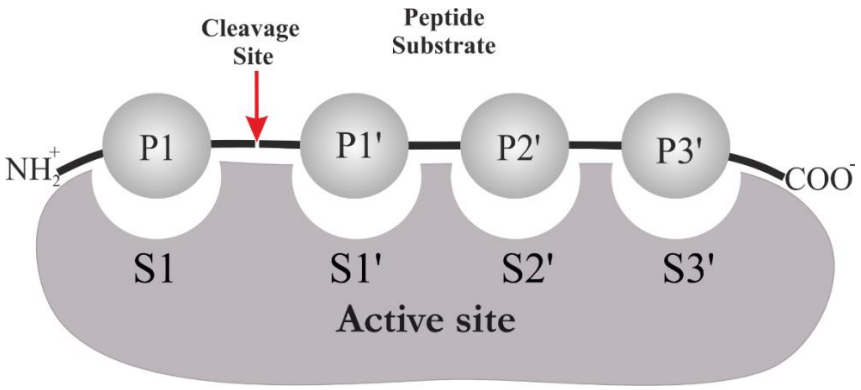

Figure S1 Active site nomenclature. Figure shows the nomenclature of active subsites (S1, S1', S2', and S3') and residues of peptide substrate (P1, P1', P2', and P3') with respect to cleavage site (Schechter and Berger nomenclature; Schechter & Berger 1967). Cleavage site is shown by a red arrow.

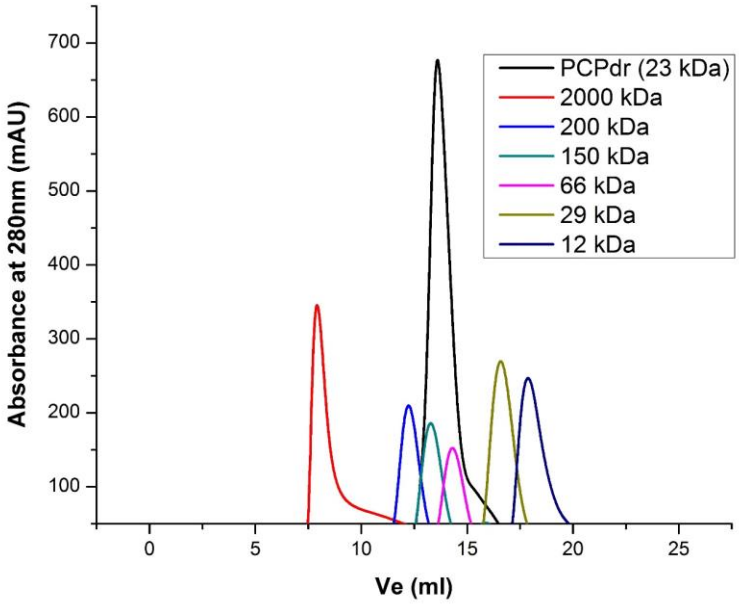

Figure S2 Gel filtration profile of PCPdr on superdex 200 10/300 GL column in buffer 20 m*M* Tris-Cl pH 8.0, 200 m*M* NaCl. The standard molecular weight markers used were 200 kDa (β amylase), 150 kDa (alcohol dehydrogenase), 66 kDa (albumin), 29 kDa (carbonic anhydrase) and 12 kDa (cytochrome C). The void volume is determined by blue dextran (red color profile) of MW~ 2000 kDa. Molecular weight for PCPdr is estimated to be about 107 kDa which is equivalent to its tetramer.

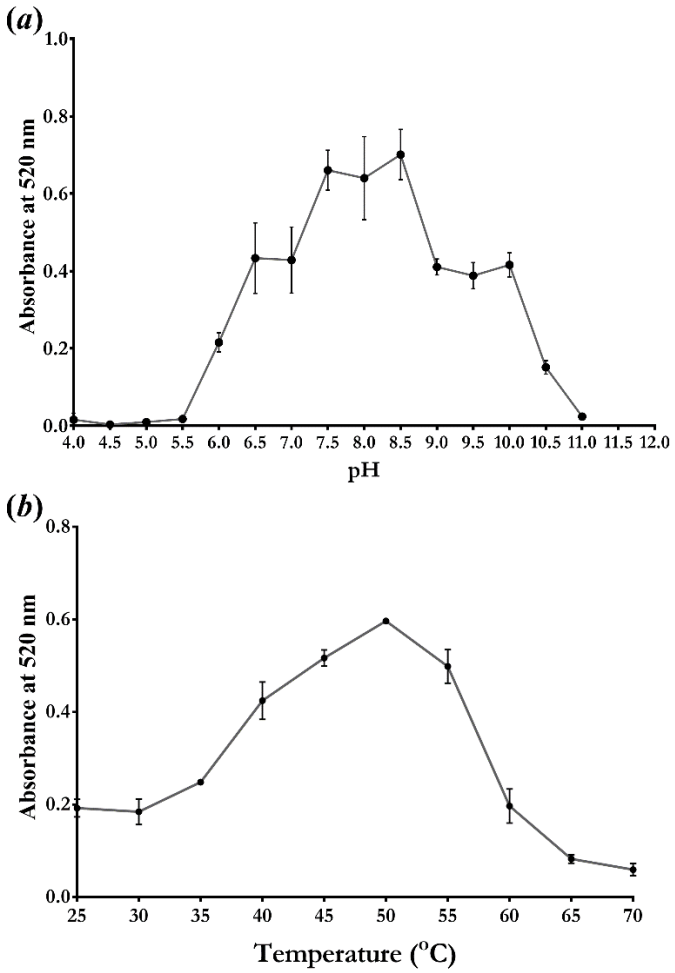

Figure S3 Optimum conditions for PCPdr enzymatic activity (*a*) Effect of pH on the activity. The assay mixture consists of enzyme (1 µg), pG–βNA (1 m*M*) but assayed with the different buffers (sodium acetate, pH 4.0 to 5.5; MES, pH 6.0 and 6.5; and Tris-Cl, pH 7.0 to 9.0 and CAPS, pH 9.5 to 11.0; each at 50 m*M*) at 50ºC. (*b*) Effect of temperature on the activity. The assay mixture has the same concentration of enzyme and substrate with Tris-Cl (50 m*M*, pH 7.5) and incubated at different temperatures.

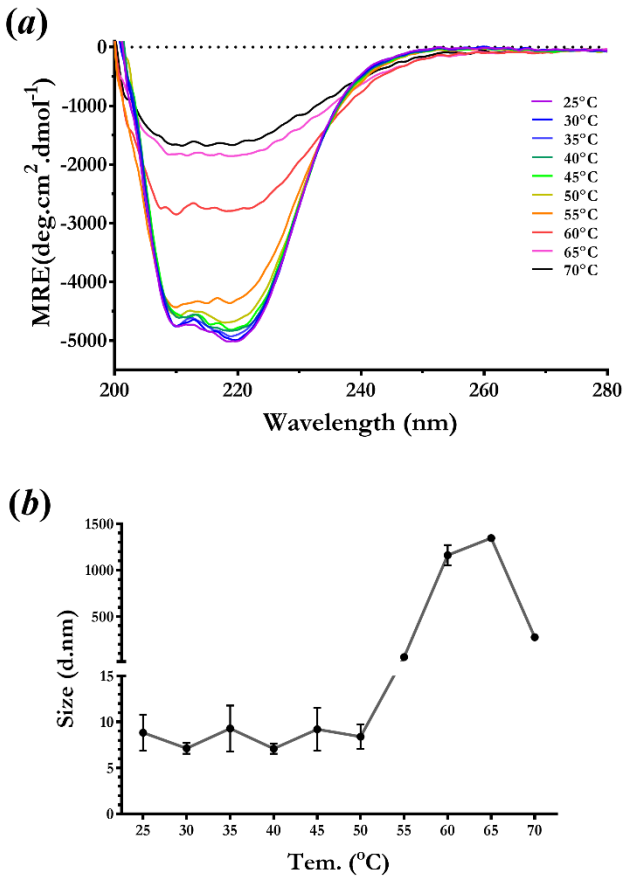

Figure S4 Effect of temperature on protein secondary structure and dimension. (*a*) CD spectra has taken with gel filtrated protein at 0.5mg/ml concentration in 20mM Phosphate buffer pH7.5 and 100mM NaCl using 2mm cuvette. Graph shows loss of secondary structure at 55ºC onwards. (*b*) DLS size distribution has measured with gel filtrated protein at 1 mg/ml concentration in 20mM Phosphate buffer pH7.5,100mM NaCl. Graph shows up to 50ºC protein was in tetrameric form. Aggregation has seen after 55ºC which observe by increase in size.

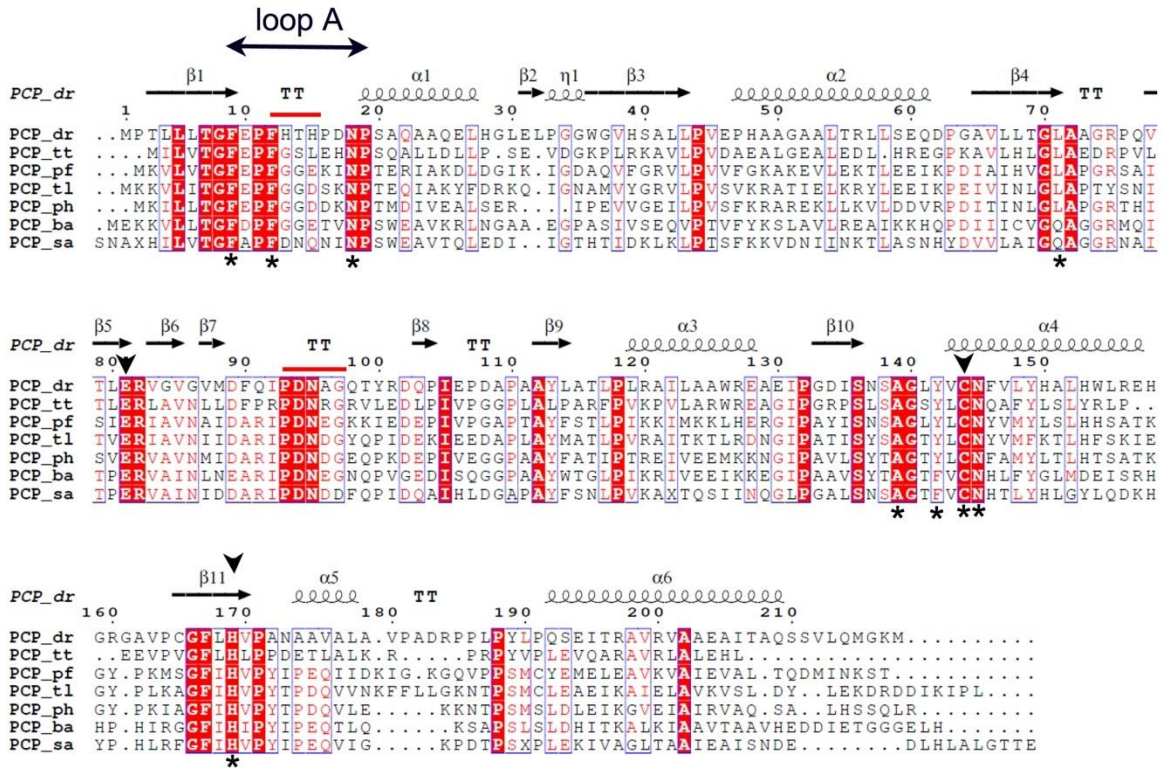

Figure S5 Multiple sequences alignment of PCPs I for which the crystal structures are known. It is overlaid by secondary structure calculated by DSSP (Touw *et. al.*, 2015). Residues marked as asterisk (*) are responsible for pyroglutamate binding while the residues of catalytic triad are marked by arrowhead. The residues of disordered loops are marked by red lines. PCP_dr (present study); PCP_tt, (PDB entry 2ebj, *Thermus thermophlius*); PCP_pf (PDB entry 2df5, *Pyrococcus furiosus*), PCP_tl (PDB entry 1a2z, *Thermococcus litoralis*) PCP_ph (PDB entry, 1iu8 *Pyrococcus horikoshii*) PCP_ba (PDB entry 1aug, *Bacillus amyloliquefaciens*) PCP_sa (PDB entry 3giu, *Staphylococcus aureus*)

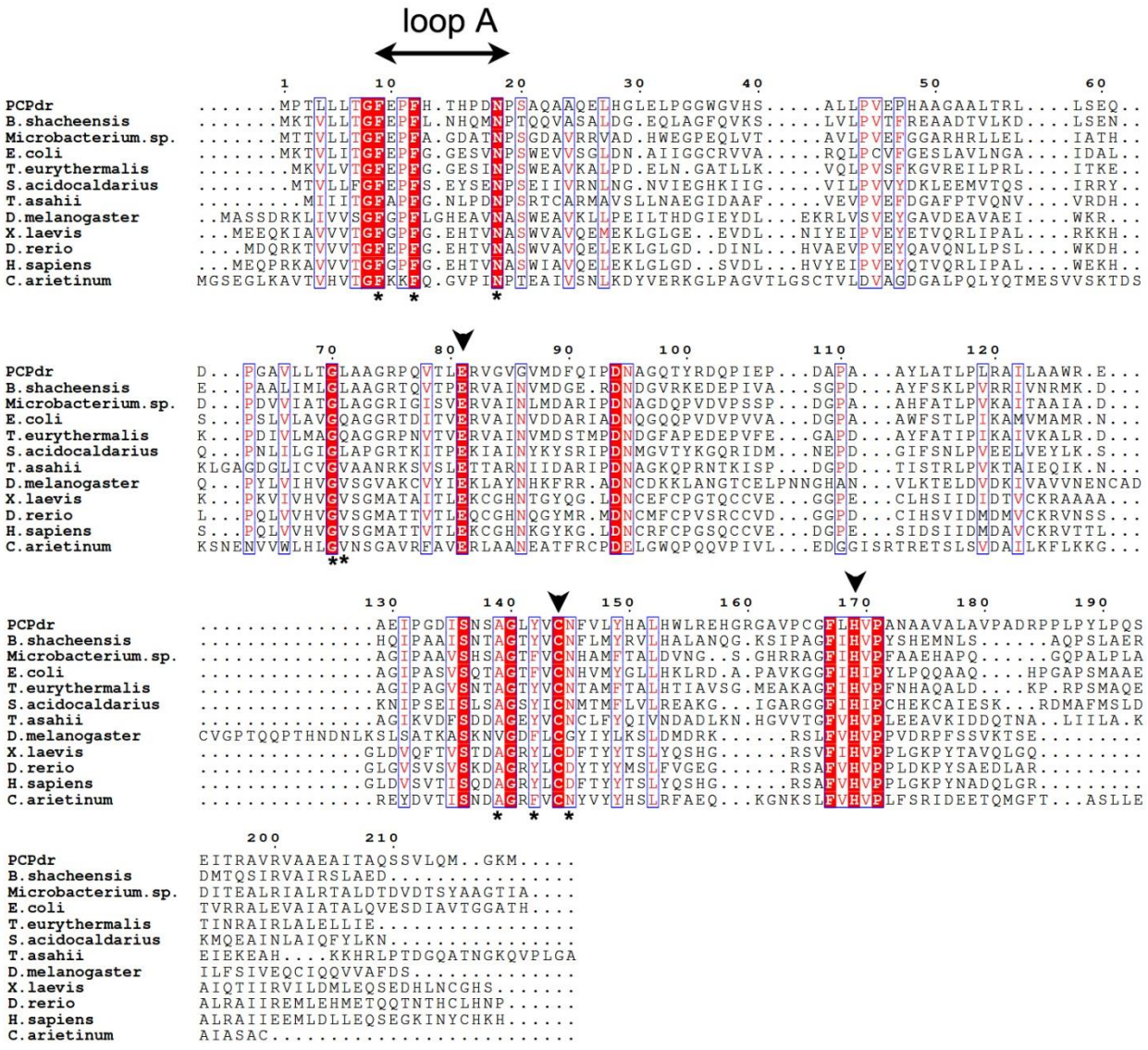

Figure S6 Conservation of PCPs I in different phyla. Residues marked as asterisk (*) are responsible for pyroglutamate binding and the residues of catalytic triad are marked with arrowhead. **PCPdr** (present study) **Fermicutes,** *Bacillus shacheensis* (WP_059103375); **Actinobacteria,** *Microbacterium sp. cf332* (SDQ83557); **Proteobacteria,** *Escherichia coli* (CDL36393); **Thermococci,** *Thermococcus eurythermalis* (WP_050002317.1); **Thermoprotie,** *Sulfolobus acidocaldarius* (WP_011278588.1); **Tremellomycetes,** *Trichosporon asahii* (XP_014179077.1); **Insecta,** *Drosophila melanogaster* (NP_730035.1); **Amphibia,** *Xenopus laevis* (XP_018110403.1); **Pieces,** *Danio rerio* (NP_001018362.1) **Mammalia,** *Homo sapiens*; (NP_060182.1); **Plants,** *Cicer arietinum* (XP_012573830.1).

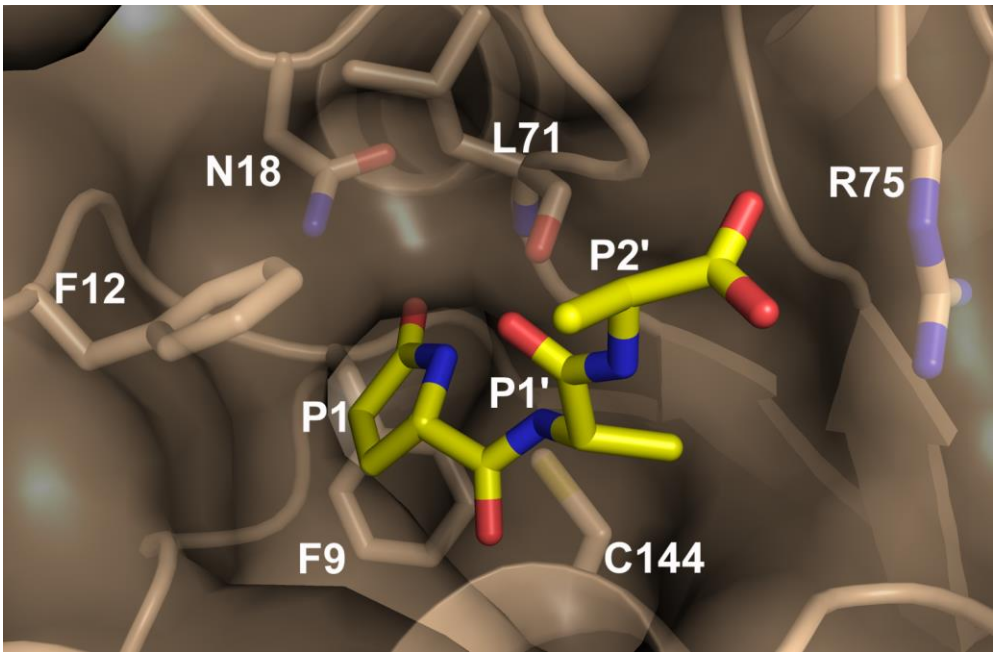

Figure S7 Modeling of tripeptide (pG-Ala-Ala) into the active site of PCPdr. Tripeptide (pG-Ala-Ala) was modeled manually into the active site based on orientation of bound pG in the PCPdr-pG structure. Key residues of S1 subsite are shown in sticks. The tripeptide is shown in yellow sticks.

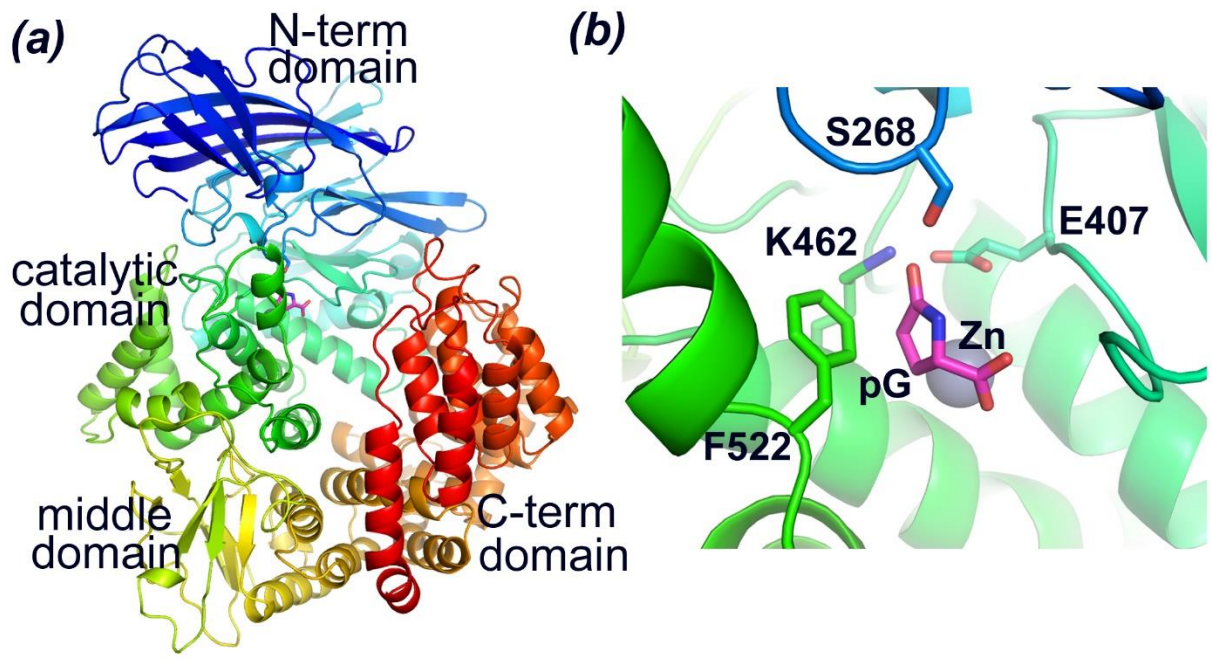

Figure S8 Modeling of human PCP II. (*a*) Structure of human PCP II modeled using porcine aminopeptidase N as a template (PDB entry 4naq) is shown in cartoon. pG (magenta sticks) manually modelled into active site based on poly-Ala substrate bound to template model is shown in magenta sticks. (*b*) The possible residues responsible for pG binding are shown in sticks. Modeled pG residue is shown in magenta sticks.

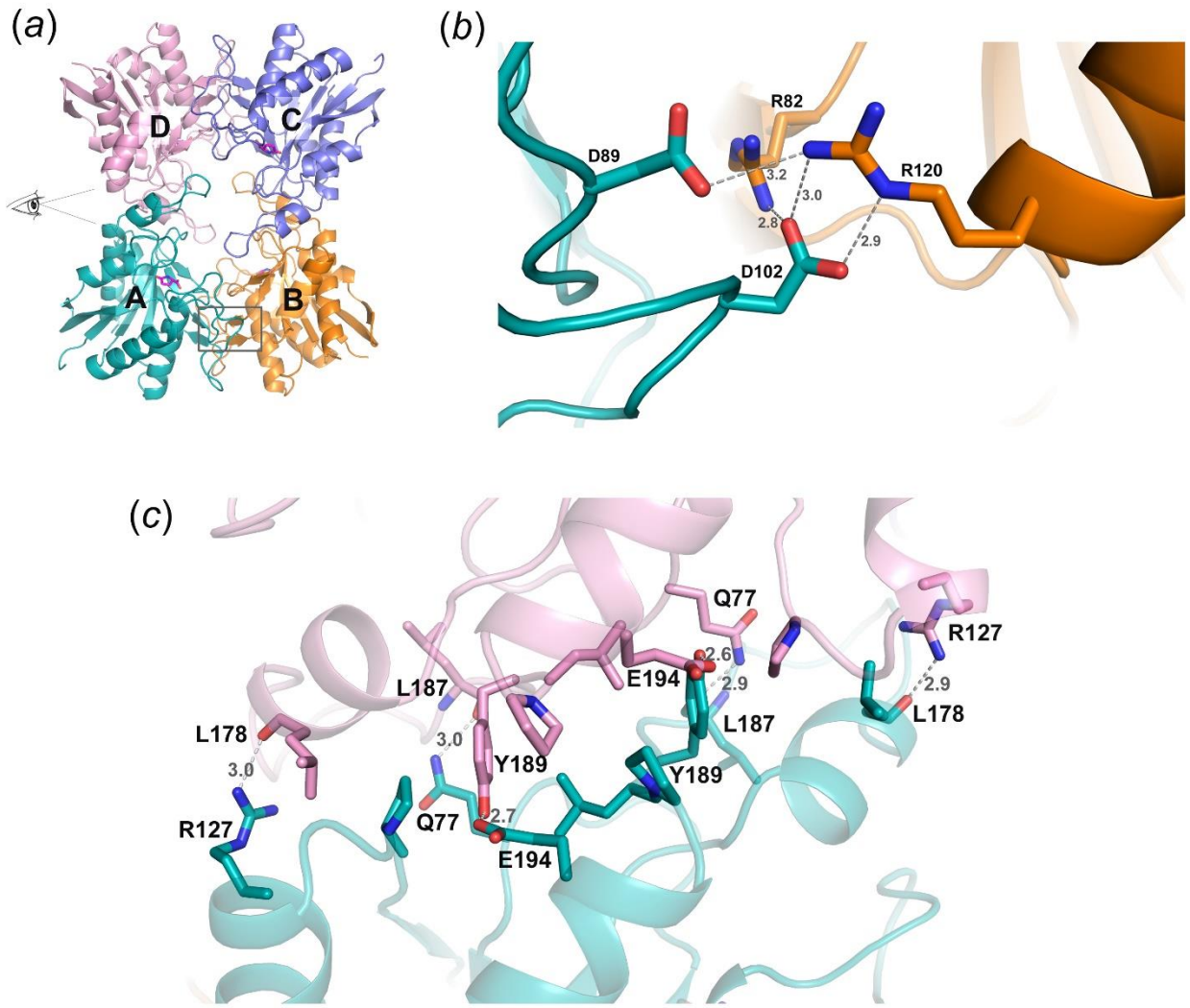

Figure S9 The interactions between protomers in a tetramer of PCPdr. (*a*) A PCPdr tetramer is shown. There are basically two types of major interactions are found in a tetramer viz. between subunit A and D and between subunit A and B. (*b*) The notable salt bridges between the subunit A and B are shown, marked by rectangle in fig. S9a (*c*) The hydrogen bonding interactions between subunit A and D are shown. The orientation of the protein is indicated by eye view in fig. S9a.

References

Schechter, I. & Berger, A. (1967). *BBRC*, 27, 157–162.

Touw, W. G., Baakman, C., Black, J., Beek, T. A., Krieger, E., Joosten, R. P., & Vriend, G. (2015) *Nucl. acids Res.* 43, 364-368.